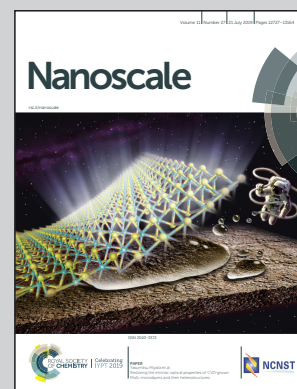


Showcasing research from the group of Professor Yu-Ming Zheng, CAS Key Laboratory of Urban Pollutant Conversion, Institute of Urban Environment, Chinese Academy of Sciences, China.

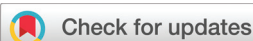
Polymer induced one-step interfacial self-assembly method for the fabrication of flexible, robust and free-standing SERS substrates for rapid on-site detection of pesticide residues

Gold nanoparticles (AuNPs) slowly rose to the water/cyclohexanone interface and self-assembled into orderly layers, when polyvinyl chloride (PVC) cyclohexanone solution was added to the top of the AuNP solution. With the cyclohexanone evaporation, a fresh thin PVC film with the orderly assembled and half-embedded AuNPs was formed at the interface.

As featured in:



See Lu-Bin Zhong, Yu-Ming Zheng *et al.*, *Nanoscale*, 2019, **11**, 12829.

Cite this: *Nanoscale*, 2019, **11**, 12829

# Polymer induced one-step interfacial self-assembly method for the fabrication of flexible, robust and free-standing SERS substrates for rapid on-site detection of pesticide residues†

Peng Wu,<sup>a</sup> Lu-Bin Zhong,<sup>b</sup> Qing Liu,<sup>a,d</sup> Xi Zhou<sup>e</sup> and Yu-Ming Zheng<sup>b</sup>

We have demonstrated a one-step approach for the fabrication of flexible, robust, reproducible and free-standing SERS substrates (AuNPs/polyvinyl chloride (PVC) film) through a polymer induced interfacial self-assembly method. In this method, the polymer (PVC) plays dual roles, that is, inducing the interfacial self-assembly of nanoparticles and fixing the assembled nanostructure in the PVC matrix. As the assembled nanoparticles are orderly half-embedded in the PVC film, the AuNPs/PVC film exhibits outstanding reproducibility and stability. In addition, the film could be easily regenerated by rinsing with NaBH<sub>4</sub> solution. As a proof of concept, the film was directly wrapped on an apple surface for *in situ* detection of pesticide residues, and a detection limit of 10 ng cm<sup>-2</sup> thiram was achieved. Furthermore, rapid on-site and *in situ* detection of multi-pesticide residues has been proved to be feasible with the aid of a portable Raman spectrometer. Due to its simple preparation, good reliability, outstanding stability and reusability, the AuNPs/PVC film has great potential in practical applications.

Received 3rd April 2019,  
Accepted 20th May 2019

DOI: 10.1039/c9nr02851j

rsc.li/nanoscale

## Introduction

With the rapidly growing population, it is estimated that global food production will have to be boosted by 70% by 2050 to meet people's basic needs.<sup>1</sup> Crops are nevertheless vulnerable to pests and are severely affected by weeds. It was reported that global food production would be decreased by 35–40% without the use of pesticides.<sup>2</sup> As a result, pesticides are used extensively and excessively in agricultural practices, leading to severe pesticide residues in the agricultural products. These pesticide residues might seriously threaten the ecological system and human health.<sup>2</sup> According to the World Health Organization (WHO), approximately 3 000 000 pesticide poi-

sonings occur every year, resulting in 220 000 deaths worldwide.<sup>1</sup> Therefore, in order to ensure an adequate supply of safe food, it is essential to rapidly identify and detect potential pesticide residues in agricultural products before they are sold.

Conventional methods for pesticide detection are mainly based on chromatographic techniques, including high performance liquid chromatography (HPLC), gas chromatography–mass spectrometry (GC-MS) and thin-layer chromatography (TLC). Although these methods have high measurement accuracy, they require high experimental cost and sophisticated pretreatment.<sup>3</sup> Recently, some novel detection techniques have emerged and been developed, such as, colorimetry, electrochemistry, fluorescence analysis and surface enhanced Raman spectroscopy (SERS), *etc.*<sup>4,5</sup> Owing to its superior advantages, including non-destructive data acquisition, unique spectroscopic fingerprints, simple sample preparation, and ultrahigh sensitivity, SERS has been proved to be a promising analytical technique.<sup>6–9</sup>

In the past decade, SERS technique has been extensively applied in the detection of trace contaminants.<sup>5,10,11</sup> For example, Liu *et al.* reported the core-shell Au@AgNPs colloid as a Raman amplifier for the detection of several pesticide residues at various fruit peels.<sup>10</sup> Mao *et al.* assembled gold nanorods on silicon wafer for the detection of drugs in human urine.<sup>11</sup> Metal NP colloids employed SERS substrates have a simple preparation process; however, the stability and reproducibility of SERS signals still face great challenges. To address

<sup>a</sup>CAS Key Laboratory of Urban Pollutant Conversion, Institute of Urban Environment, Chinese Academy of Sciences, 1799 Jimei Road, Xiamen 361021, China.  
E-mail: lbzhong@iue.ac.cn, ymzheng@iue.ac.cn; Tel: +86-592-6190590, +86-592-6190785

<sup>b</sup>CAS Center for Excellence in Regional Atmospheric Environment, Institute of Urban Environment, Chinese Academy of Sciences, Xiamen 361021, China

<sup>c</sup>University of Chinese Academy of Sciences, 19A Yuquan Road, Beijing 100049, China

<sup>d</sup>Fujian Provincial Key Laboratory of Ecology-Toxicological Effects & Control for Emerging Contaminants, Putian University, Putian 351100, China

<sup>e</sup>Department of Biomaterials, College of Materials, Xiamen University, Xiamen 361005, China

† Electronic supplementary information (ESI) available. See DOI: 10.1039/c9nr02851j

these problems, metal NPs are regularly assembled on silicon wafers or glass sides as SERS substrates. Nevertheless, these hard templates are rigid and heavy, which brings enormous inconvenience in practical applications, especially in storage, transportation and detection of contaminants on irregular objects.

Recently, great efforts were dedicated to fabricate flexible and semitransparent SERS substrates to promote SERS application in real life.<sup>12–22</sup> For instance, a flexible and sticky SERS substrate was constructed by placing a concentrated AuNP solution dropwise onto a commercial tape, which was able to directly extract and detect target molecules.<sup>17</sup> Through deposition of Ag onto a 3D polydimethylsiloxane (PDMS) nanotactile array, Wang *et al.* developed a flexible gecko-inspired SERS substrate to detect pesticide residues.<sup>19</sup> Koh *et al.* reported an M13 bacteriophage/silver nanowire as a flexible SERS substrate for sensitive and selective pesticide detection.<sup>21</sup> Although these flexible SERS substrates exhibit impressive advantages compared to the hard SERS substrates, the complex preparation process and difficulty in recycling significantly increase the detection cost. In addition, robustness of the substrates is still a huge challenge, as the SERS-active NPs are apt to be separated from the substrates in long-term applications, especially under harsh conditions, such as ultrasound or rubbing.

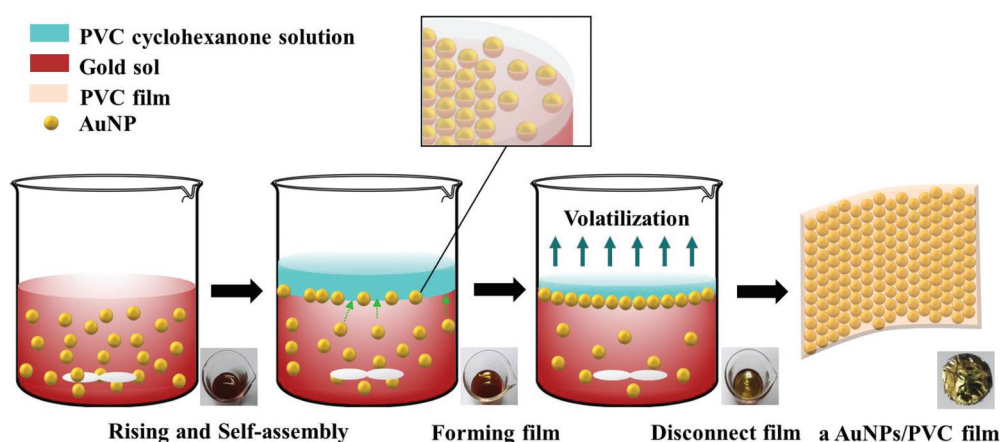
We previously developed a simple method to fabricate a flexible and semitransparent SERS substrate, the AuNPs/PMMA/PE, which was successfully used to detect residual malachite green in fish and can be easily regenerated.<sup>23</sup> Although the preparation methods are simpler compared to other SERS substrates, polyethylene (PE) film was required to support the AuNPs/PMMA substrate due to the weak mechanical robustness of PMMA and ethanol was also needed to induce the rise and assembly of AuNPs at the aqueous/organic interface.<sup>8,23</sup> In this work, we further improve the strategy to fabricate a novel free-standing SERS substrate with excellent flexibility and robustness. Moreover, the overall preparation process was simpler and the cost was remarkably reduced, as

shown in Scheme 1. AuNPs slowly rose to the water/cyclohexanone interface and self-assembled into orderly layers when polyvinyl chloride (PVC) cyclohexanone solution was added to the top of the AuNP solution. With the cyclohexanone evaporation, a fresh thin PVC film was formed at the interface with the assembled AuNPs half-embedded which was fixed by the physical shrinking force of PVC. PVC was chosen due to its excellent flexibility, high optical transparency, and clear SERS background. Furthermore, PVC cyclohexanone solution can directly induce the rise and assembly of AuNPs, thus, was much more convenient than previous methods which often require an inducing agent such as ethanol.<sup>24</sup> Finally, a flexible, robust and free-standing AuNPs/PVC film was obtained. The AuNPs/PVC film was tested in different conditions and exhibited excellent reproducibility, outstanding stability and good regenerability. With the aid of a portable Raman spectrometer, on-site and *in situ* SERS detection of multi-pesticide residues can be achieved by directly wrapping the film on the surface of an irregular object, such as apple.

## Experimental section

### Chemical reagents

Tetrachloroauric (III) acid hydrate ( $\text{AuCl}_3 \cdot \text{HCl} \cdot 4\text{H}_2\text{O}$ ), trisodium citrate dehydrate ( $\text{C}_6\text{H}_5\text{Na}_3\text{O}_7 \cdot 2\text{H}_2\text{O}$ , 99.0%), ethanol ( $\text{C}_2\text{H}_6\text{O}$ , 99%), sodium borohydride ( $\text{NaBH}_4$ , 99%), hydrogen chloride, nitric acid, sodium hydroxide (98%) were purchased from Sinopharm Chemical Reagent Co., Ltd (Shanghai, China). Thiram ( $\text{C}_6\text{H}_{12}\text{N}_2\text{S}_5$ , 97%), cyclohexanone ( $\text{C}_6\text{H}_{10}\text{O}$ , 99%), and parathion-methyl solution ( $\text{C}_8\text{H}_{10}\text{NO}_5\text{PS}$ ) were obtained from Aladdin Chemical Reagent Co., Ltd (China). 4-Aminothiophenol (4-ATP,  $\text{C}_6\text{H}_7\text{NS}$ , 97%) was purchased from Sigma-Aldrich. All reagents mentioned above were of analytical grade and used without further purification. PVC was procured from Ningxia Yinglite Chemicals Co., Ltd. Apples were bought from a local supermarket. Ultrapure water ( $18.2 \text{ M}\Omega \text{ cm}$ ) was obtained from a Millipore Milli-Q Advantage A10 water purifi-



Scheme 1 Schematic diagram of fabricating a AuNPs/PVC film.

cation system and was used for all aqueous solution preparations.

### Synthesis of AuNPs

AuNPs with a diameter of 50 nm were prepared according to the method reported in our previous work with minor modification.<sup>23</sup> In a typical synthesis, 1 mL of sodium citrate solution (34 mmol L<sup>-1</sup>) was quickly added to 99 mL of aqueous HAuCl<sub>4</sub> solution (0.243 mmol L<sup>-1</sup>) that was stirred under boiling conditions, and the mixture was boiled for 3 min to obtain a wine-red solution. Another 1 mL of sodium citrate solution (34 mmol L<sup>-1</sup>) and 1 mL of HAuCl<sub>4</sub> solution (24.3 mmol L<sup>-1</sup>) were then successively added into the mixture every 30 s, and this step was repeated 3 times. The solution was heated for another 5.5 min, then the heating was stopped, and the reaction mixture was cooled down to room temperature. The mean size of the as-prepared AuNPs was 50 ± 5 nm.

AuNPs with a diameter of 20 nm were prepared by one-step reduction using sodium citrate as both a reducing agent and a capping agent. First, 2 mL of sodium citrate solution (34 mmol L<sup>-1</sup>) was quickly added to 99 mL of aqueous HAuCl<sub>4</sub> solution (0.243 mmol L<sup>-1</sup>) that was stirred under boiling conditions. And the mixture was boiled for 5 min to give a light red solution. After that, the mixture was cooled down to room temperature. The mean size of the prepared AuNPs was 20 ± 2 nm.

### Fabrication of the AuNPs/PVC film

First, the as-synthesized AuNP (15 mL) solution was taken into a beaker, and then 4 mL PVC cyclohexanone solution of a desired concentration was added into the beaker slowly along the inner wall. Due to the immiscibility of water and cyclohexanone, a clear water/cyclohexanone interface was formed. After that, the mixed solution was gently stirred by a magnetic stirrer. Meanwhile, the AuNPs gradually rose to the water/cyclohexanone interface and self-assembled into orderly and compact AuNP layers at the interface. A thin PVC template was simultaneously formed on the aqueous solution surface due to the evaporation of cyclohexanone. As a result, the self-assembled AuNP layers were fixed in the newborn PVC template. When the cyclohexanone completely evaporated, the AuNPs/PVC film was formed and could be retrieved from the solution surface. The detailed process is shown in Scheme 1.

### SERS performance of the AuNPs/PVC film

To evaluate reproducibility, stability and the enhancement factor of the AuNPs/PVC film, the film was firstly immersed in 4-ATP solution (0.1 mmol L<sup>-1</sup>) for 30 min. The AuNPs/PVC film was then rinsed with ethanol to remove the unbound 4-ATP molecules and dried at room temperature to evaporate the ethanol. Finally, a monolayer of 4-ATP was adsorbed on the AuNPs/PVC film surface.

### Detection of pesticide residues on apple surface

Apples were rinsed thoroughly using deionized water before use. Sample 1 was detected by a laboratory Raman spec-

troscopy. For more reliable SERS detection, apple peels were taken from cleaned apples using a fruit knife and cut into nearly uniform square pieces of ~1 cm<sup>2</sup>. Then, 10 μL of thiram solution with different concentrations was directly added onto the surface of the apple peel. After natural evaporation at room temperature, 10 μL of ethanol was added onto the pretreated apple peel to extract the pesticide. Subsequently, the AuNP/PVC film was pasted onto the surface of the apple peel for further SERS analysis by laboratory Raman spectroscopy.

Sample 2 was detected using a portable Raman spectrometer. Thiram (10 μL, 20 mg L<sup>-1</sup>), parathion-methyl (10 μL, 50 mg L<sup>-1</sup>), or their mixture solution was placed onto the apple surfaces dropwise, respectively. When these solutions were evaporated fully, 10 μL ethanol was then added onto the apple surfaces to extract the analyte. Subsequently, an AuNP/PVC film was pasted to the apple surfaces, and Raman signals were collected *in situ* from the film *via* a portable Raman spectrometer.

### Characterization

Raman spectroscopy measurements were carried out using a LabRAM Aramis Raman spectrometer (Horiba Jobin Yvon, France) with 785 nm, 633 nm and 532 nm laser excitation sources, and the corresponding power was 0.27 mW, 0.10 mW and 0.21 mW, respectively. The Raman spectra were acquired using a 50× objective lens, a 5 s exposure time and two accumulations. Absorption spectra were measured using a UV-2450 UV-VIS spectrophotometer (Shimadzu, Japan) in 1 cm optical path quartz cuvettes. Scanning electron microscopy (SEM) images were obtained using a S-4800 field emission scanning electron microscope (Hitachi, Japan) operating at an accelerating voltage of 50 kV. The AuNPs/PVC film was treated with low-pressure air plasma using a PDC-002 plasma cleaner (Harrick Plasma, USA) to remove the surface excess PVC and trace impurities for several seconds prior to Raman analysis. A portable Raman spectrometer (Advantage Raman Series, DeltaNu) was used for on-site pesticide residue detection.

## Results and discussion

### Characterization of the AuNPs/PVC film

The UV-vis spectra in Fig. 1a displayed that the monodisperse AuNP solution with different diameters exhibited different surface plasma absorption bands. The maximum absorption wavelength of the 20 nm AuNPs was ~520 nm, while that of the 50 nm AuNPs was ~564 nm. Compared with the monodisperse AuNPs in solution, the UV-vis spectra of both kinds of AuNPs/PVC films changed remarkably. The absorption peak of the AuNPs/PVC film with 20 nm sized AuNPs, denoted as the AuNPs<sub>20</sub>/PVC film, red-shifted from 520 to 675 nm, while a new peak at around 880 nm appeared at the AuNPs/PVC film with 50 nm sized AuNPs, denoted as the AuNPs<sub>50</sub>/PVC film. These changes may be attributed to the strong interparticle electronic coupling when the AuNPs were brought closely, suggesting that the AuNPs were assembled on the PVC tem-

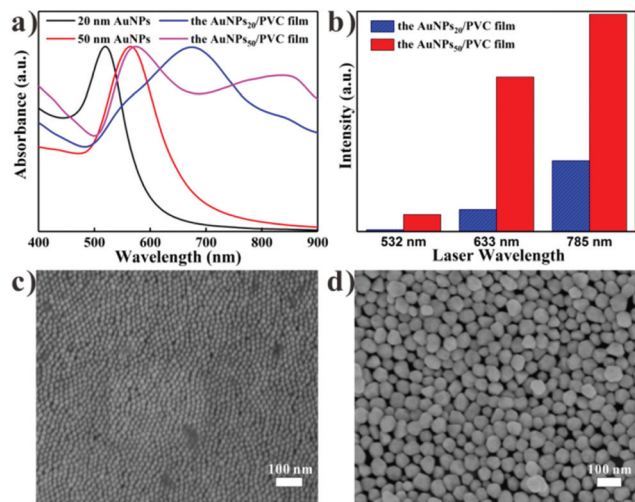


**Fig. 1** (a) UV-vis absorption spectra of the AuNP solution and the AuNPs/PVC films with 20 nm and 50 nm AuNPs. (b) Comparison of SERS signal intensities collected with the AuNPs<sub>20</sub>/PVC film and the AuNPs<sub>50</sub>/PVC film under diverse lasers (the intensity has been normalized due to different laser powers). SEM images of (c) the AuNP<sub>20</sub>/PVC film and (d) the AuNPs<sub>50</sub>/PVC film. Integration time = 5 s.

plate. SEM images of the AuNPs/PVC films were observed to further confirm this hypothesis. As expected, both kinds of AuNPs were self-assembled into ordered layers on the PVC template (Fig. 1c and d). These densely ordered layers created a high density of hot spots that could significantly amplify the Raman signal of analytes adsorbed on its surface and improve the detection sensitivity.

### Optimization of AuNP size and laser wavelength

To optimize the SERS enhancement effect, AuNPs/PVC films with different AuNP diameters were tested under diverse laser wavelengths. 4-ATP was used as a probe molecule here to evaluate the SERS performance of the AuNPs/PVC films due to forming a strong Au-S bond with the AuNPs. The characteristic peak of 4-ATP at 1078  $\text{cm}^{-1}$  was used as a quantitative peak. The measurement showed that the AuNPs<sub>50</sub>/PVC film exhibited better performance than the AuNPs<sub>20</sub>/PVC film, and the best laser wavelength was 785 nm (Fig. 1b and Fig. S1†). Consequently, the AuNPs<sub>50</sub>/PVC film was selected as the SERS substrate and 785 nm laser was adopted as the optimum excitation source in the following study.

### Optimization of the AuNPs/PVC film thickness

Light weight and flexibility, which are beneficial for storage, transportation and detection of contaminants on irregular objects, are two key factors of SERS substrates in practical applications. To obtain a more flexible and ultralight film, the AuNPs/PVC film should be as thin as possible. However, extremely thin AuNPs/PVC films would be prone to fracture and unlikely to be free-standing. Therefore, the thickness of the film should be optimized. Fortunately, the thickness of the AuNP/PVC film can be easily adjusted by regulating the content of

PVC (Fig. S2†). Preliminary experimental results indicated that the AuNPs/PVC film could not maintain its free-standing nature when the content of PVC was lower than  $1.2 \text{ mg cm}^{-2}$ , and became rigid when more than  $12.4 \text{ mg cm}^{-2}$  PVC was added. Herein, PVC contents from  $1.2$  to  $12.4 \text{ mg cm}^{-2}$  were adopted in this work, and the corresponding UV-vis spectra of AuNP/PVC films were recorded. The absorption peak intensity at 564 nm gradually increased with the increment of PVC content; meanwhile, a new absorption band emerged at a high wavelength and became increasingly obvious (Fig. 2a). SERS signal intensity measurement results indicated the SERS intensity increased with the increasing PVC content and reached a maximum when  $12.4 \text{ mg cm}^{-2}$  PVC was used (Fig. 2b). However,  $6.2 \text{ mg cm}^{-2}$  PVC was adopted instead in view of better flexibility, and the optimal thickness of the AuNPs/PVC film was  $\sim 178 \mu\text{m}$  (Fig. S2c†). The flexibility of the film was characterized clearly *via* bending and folding it, as shown in Fig. 2c. Like a paper, the AuNPs/PVC film can be easily rolled around a needle. Furthermore, the film was unbroken even when it was folded four times into a small rectangle. Double-sided Raman signals of the  $6.2 \text{ mg cm}^{-2}$  AuNPs/PVC film were collected (Fig. S3a†). There was no significant difference in SERS signal intensities of both sides, which was in accordance with a previous work reported by Wang *et al.*<sup>25</sup> In addition, the PVC template had an outstanding advantage, that is, the SERS background is clear due to its low Raman cross-section, as shown in Fig. S3c and d.† Thus, the interference of the background signals would be minimized, which is beneficial for analyte detection.

### Reproducibility, sensitivity and stability of the AuNPs/PVC film

Reproducibility, sensitivity and stability are crucial parameters for characterizing the performance reliability of a SERS substrate. A monolayer of 4-ATP adsorbed on the AuNPs/PVC film surface was used to evaluate these performances. The optical micrograph in Fig. 3a indicated that the AuNPs/PVC film had a uniform surface over  $2500 \mu\text{m}^2$ . Furthermore, the Raman

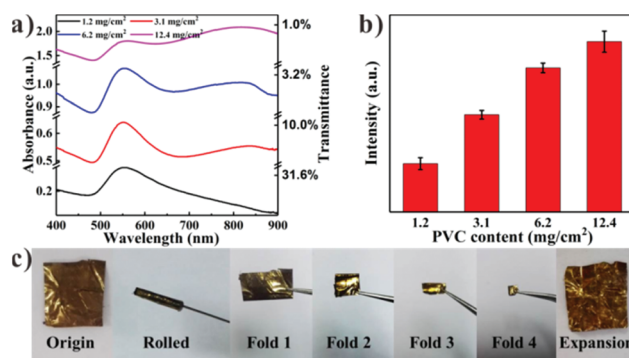


**Fig. 2** (a) UV-vis spectra of the AuNPs/PVC films with different PVC contents. (b) Comparison of Raman intensities of the AuNPs/PVC films in the front side with different PVC contents. (c) Photographs of the AuNP/PVC film before and after rolling and folding ( $6.2 \text{ mg cm}^{-2}$  PVC). The diameter of needle is 0.5 mm. Laser wavelength = 785 nm; laser power = 0.27 mW; integration time = 5 s.

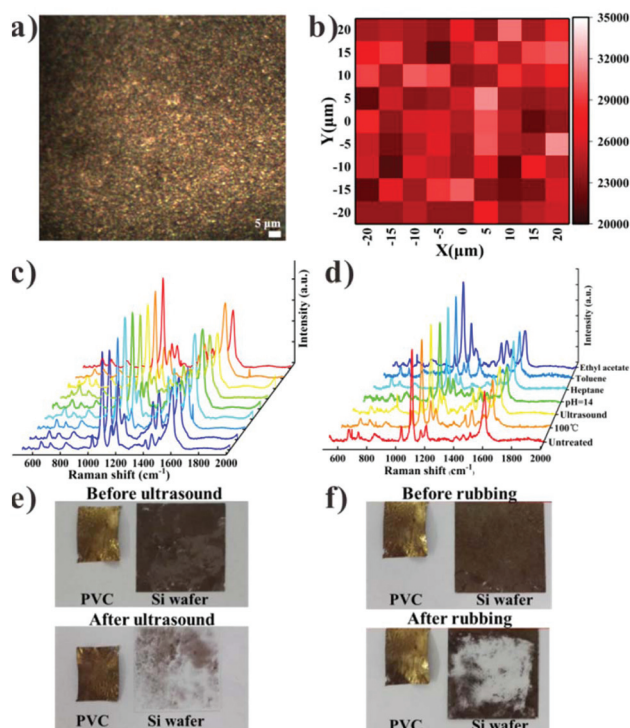


**Fig. 3** (a) Optical micrograph obtained by a Raman spectrometer and (b) the corresponding SERS intensity distribution mapping ( $40 \times 40 \mu\text{m}$ ) at  $1078 \text{ cm}^{-1}$  of 4-ATP adsorbed on the AuNPs/PVC film. (c) SERS spectra of 4-ATP collected from 8 different AuNPs/PVC films. (d) SERS signal of the AuNPs/PVC film before and after treatment with organic solvents (ethyl acetate, heptane and toluene) and strong base (NaOH), heating at  $100 \text{ }^\circ\text{C}$ , or under ultrasound. (e) Comparison of the AuNPs/PVC film and a traditional Si template SERS substrate before and after ultrasound treatment. (f) Comparison of the AuNPs/PVC film and a traditional Si template SERS substrate before and after rubbing with filter paper. Laser wavelength =  $785 \text{ nm}$ ; laser power =  $0.27 \text{ mW}$ ; integration time =  $5 \text{ s}$ .

signal intensity mapping from 4-ATP adsorbed on the AuNPs/PVC film was recorded to further demonstrate the uniformity across the entire film (Fig. 3b). According to the counted values of all points at  $1078 \text{ cm}^{-1}$ , a relative standard deviation (RSD) of 10.24% was acquired. Such an excellent reproducibility of SERS signals may be attributed to the ordered assembly of the AuNP layers. In addition, the batch-to-batch reproducibility testing was also carried out by detecting SERS spectra of 4-ATP from 8 batches of AuNPs/PVC films (Fig. 3c). The RSD of signal intensities at  $1078 \text{ cm}^{-1}$  on 8 different films is 12.54%, revealing a good batch-to-batch reproducibility of the AuNP/PVC film. These results clearly demonstrated the excellent SERS reproducibility of the AuNPs/PVC film.

To quantitatively characterize the SERS activity, the enhancement factor (EF) was calculated according to the following formula:  $\text{EF} = (I_{\text{SERS}}/N_{\text{SERS}})/(I_{\text{NR}}/N_{\text{NR}})$ .<sup>26</sup> The result showed that the EF reached  $3.7 \times 10^6$  based on the values of all points in Fig. 3b (the details for EF calculation are provided in the ESI†), revealing a remarkably enhanced performance of the film. To obtain additional insight into the above experimental observations, the electromagnetic field responses were

studied using the 3D-FDTD method.<sup>27</sup> As described above, a nanostructure composed of seven AuNPs with diameters of  $50 \text{ nm}$  was modelled on a computer (Fig. S4†). The distance of the interparticle gap was  $3 \text{ nm}$ , and the nanostructure was subjected to irradiation with  $785 \text{ nm}$  laser light. The intensity distribution of calculated electric field ( $|E/E_0|^4$ ) was used as a function. Most SERS signals arose from hot spots of the interparticle gap as shown in Fig. S4.† When a laser light was irradiated in perpendicular polarization, the maximum surface EF was about  $1 \times 10^7$ . The experimental enhancement was lower than the simulated EF. The reason was that the enhancement in the interparticle gap was maximum in the nanostructure, while the experimental result was the average local field enhancement over the entire probe area rather than a point. Thus, the experimental enhancement was an order of magnitude smaller than the simulated value. To further increase the EF, the AuNPs/PVC film can be further treated by a plasmon cleaner to remove excess PVC and expose more hot spots.<sup>15</sup> As shown in Fig. S5,† higher signal intensities were obtained after plasma treatment. The peak intensity of 4-ATP at  $1078 \text{ cm}^{-1}$  increased by 66.00% and 2.38% after the plasma treatment for 30 s and 60 s, respectively. The decrease in the Raman signal for 60 s plasma treatment may be ascribed to the destruction of the film due to excessive plasma treatment.

Considering various detection environments in practical applications, the stability of the AuNPs/PVC film is indispensable. Thus, the AuNPs/PVC film was further tested under some harsh conditions, such as immersing in organic solvents or strong base, high temperature, ultrasound or rubbing. It was quite exciting that the SERS signal intensities of the AuNPs/PVC film did not obviously change after treatment with three organic solvents (ethyl acetate, heptane and toluene), NaOH aqueous solution ( $\text{pH} = 14$ ), high temperatures ( $100 \text{ }^\circ\text{C}$ ), and ultrasound ( $500 \text{ W}$ ) for 1 h (Fig. 3d). The results revealed that the film was extremely robust and possessed excellent stability. To simulate the friction impact between the film and the objects during the detection procedure, ultrasound and rubbing measurements were carried out. In contrast to traditional SERS substrates without the PVC template, the AuNPs/PVC film maintained good mechanical behavior without structural breakdown after ultrasound treatment or rubbing with filter paper several times (Fig. 3e and f). This prominent feature promoted a wider application of the AuNPs/PVC film in actual detection, for instance, rubbing object surfaces to enrich contaminants. In addition, permanent signal stability of the film was tested as well. Fig. S6† shows that no significant change was observed between a freshly prepared film and the same film after 3-month storages, indicating that the film was stable in air and could be used after long time storage. The above results clearly proved that the AuNPs/PVC film exhibited excellent reproducibility, high sensitivity and outstanding stability, which are vital to practical assays.

### Detection of pesticide residues on apple peels

Pesticides can effectively protect crops from pests and weeds; however, pesticide residues might severely threaten human

health. Due to its excellent flexibility and outstanding stability, the AuNPs/PVC film can be easily attached or swabbed onto the surface of random curvature without cracking, which is particularly beneficial to identify and detect pesticide residues on fruit surfaces. Thiram and parathion-methyl, two of the most commonly used pesticides in agriculture, were chosen as model contaminants in this study. In the spiked study, 10  $\mu\text{L}$  of thiram solution with different concentrations was added on the apple surface, which was then completely dried at room temperature to simulate a contaminated apple. After that, a drop of 10  $\mu\text{L}$  ethanol was sprayed on the apple surface and the AuNPs/PVC film was attached on it, followed by direct SERS signal acquisition. Fig. 4a shows that the SERS spectra collected from the film attached to the apple surfaces which

were contaminated with different concentrations of thiram. Several characteristic peaks assigned to thiram were observed, such as 551, 1140 and 1378  $\text{cm}^{-1}$ , which were attributed to  $\nu(\text{S-S})$ ,  $\rho(\text{CH}_3)$  or  $\nu(\text{C-N})$ , and  $\rho(\text{CH}_3)$ , respectively.<sup>10</sup> The prominent peak at 1378  $\text{cm}^{-1}$  was selected as the indicator. When thiram concentration decreased, the peak intensity at 1378  $\text{cm}^{-1}$  gradually diminished (Fig. 4a). The minimum detectable concentration of thiram was 10  $\text{ng cm}^{-2}$ , which is lower than the maximum residue limit of 31.3  $\mu\text{g cm}^{-2}$  for thiram in China and European Union. The result indicated that the sensitivity of the film was enough for actual application.<sup>21</sup> Raman peak intensities at 1378  $\text{cm}^{-1}$  were plotted against the natural logarithm of thiram concentrations in Fig. 4b. A satisfactory linear relationship was obtained, and the correlation coefficient was calculated to be 0.9166. This excellent correlation between peak intensities and thiram concentrations and the relatively low detection limit highlight the effectiveness of the film for on-site detection of pesticide residues.

An ideal SERS substrate should be reusable in order to effectively reduce the detection cost. Unfortunately, most of the currently reported SERS substrates are difficult to clean, especially when a strong bond, such as Au-S, is formed between analytes and SERS substrates. The reason is that ultrasound or strong cleaning agents, which can break the Au-S bond, would destroy the SERS substrates that are constructed *via* physical deposition or chemisorption as well. Since PVC served to fix the assembled AuNPs in the film, the AuNPs/PVC film can withstand strong cleaning agents and ultrasound as proved earlier. Herein, a strong reductant,  $\text{NaBH}_4$ , was used to break the Au-S bond between thiram and the AuNPs/PVC film surface to regenerate the film.<sup>28</sup> Fig. 4c clearly shows that the Raman signals collected from the AuNPs/PVC film were almost the same even after 7 cycles of regeneration. As the AuNPs/PVC film can be easily regenerated, the operating cost can be greatly reduced to broaden its applications.

To prove the feasibility of on-site detection using the developed AuNPs/PVC film, a field test was conducted with the aid of a portable Raman spectrometer (Fig. 5). No obvious Raman peaks were detected on contaminated apples, when the laser was directly shot onto it (Fig. 5a). On the contrary, two evident Raman peaks at 551  $\text{cm}^{-1}$  and 1378  $\text{cm}^{-1}$  ascribed to thiram

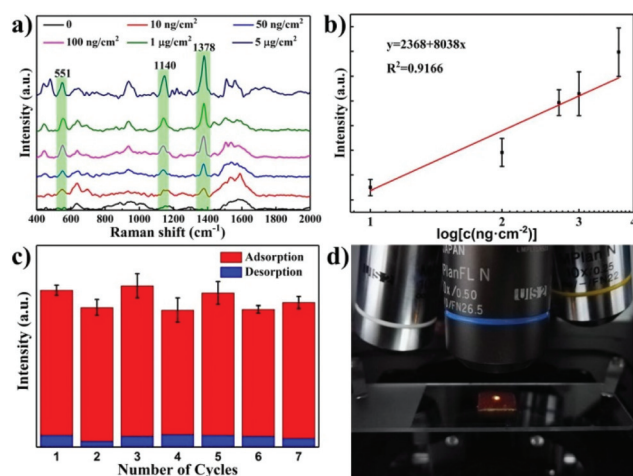


**Fig. 4** *In situ* detection of pesticide by a laboratory Raman spectrometer: (a) *In situ* detection of thiram solution with different concentrations *via* attaching the AuNPs/PVC film to the apple surfaces and illuminating from the backside (PVC template) with a 785 nm laser. (b) Quantitative calibration curve of the thiram major peak intensities at 1378  $\text{cm}^{-1}$  against the natural logarithm over their concentrations according to (a). (c) The Raman signals collected from the AuNPs/PVC film in seven successive testing–regeneration cycles. (d) Photograph of thiram detection using a laboratory Raman spectrometer with a 50 $\times$  objective lens. Laser wavelength = 785 nm, laser power = 0.27 mW, integration time = 5 s.

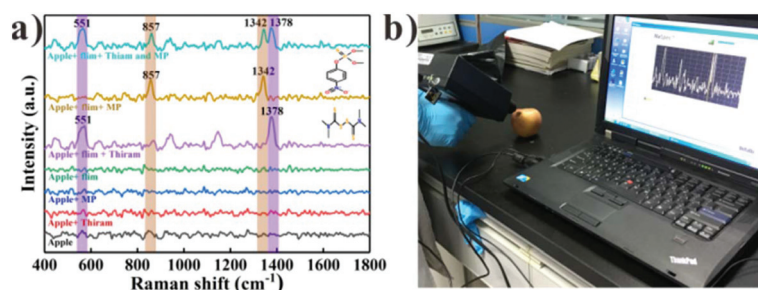


**Fig. 5** (a) Detection of thiram, parathion-methyl and their mixture with a portable Raman spectrometer. (b) Photograph of on-site and *in situ* detection of pesticides on apple surfaces.  $C_{[\text{thiram}]} = 200 \text{ ng cm}^{-2}$ ,  $C_{[\text{parathion-methyl}]} = 500 \text{ ng cm}^{-2}$ ,  $C_{[\text{multi-thiram}]} = 150 \text{ ng cm}^{-2}$ ,  $C_{[\text{multi-parathion-methyl}]} = 350 \text{ ng cm}^{-2}$ . Laser wavelength = 785 nm; integration time = 2 s.

were clearly observed on the thiram-contaminated apple to which the film was attached. Similarly, two characteristic peaks of parathion-methyl at 857  $\text{cm}^{-1}$  and 1342  $\text{cm}^{-1}$  were also detected on the parathion-methyl-contaminated apple when the film was attached to the apple surface.

Generally, to provide better protection for the crops from pests and weeds, various pesticides are often blended and used, which results in more toxic multi-pesticide residues. Due to its distinctive fingerprinting property, SERS has the ability to identify individual contaminants from complicated mixtures without pre-separation. Herein, the AuNPs/PVC film was further used to detect pesticide mixture (thiram and parathion-methyl) on apple surfaces. As shown in Fig. 5a, the typical Raman peaks of both thiram (at 551  $\text{cm}^{-1}$  and 1378  $\text{cm}^{-1}$ ) and parathion-methyl (857  $\text{cm}^{-1}$  and 1342  $\text{cm}^{-1}$ ) were distinctively discerned throughout the spectrum. These results clearly demonstrated that the AuNPs/PVC film can be employed for on-site and *in situ* detection of multi-pesticide residues in real samples, which has promising application prospects in food safety, environmental monitoring, etc.

## Conclusions

In summary, a simple preparation method was developed for the fabrication of a low cost, flexible, robust and reusable AuNPs/PVC film, which demonstrated great potential and advantages in serving as a SERS substrate for on-site and *in situ* multi-pesticide residue detection. Differing from the reported preparation methods, which often require two or more steps, the method developed can fabricate flexible SERS substrates in one step, in which PVC plays the most crucial role. PVC not only can induce the interfacial self-assembly of AuNPs, but also fixes the AuNPs in the polymer matrix to form half-embedded AuNPs/PVC film. Due to the rigid fixation, the AuNPs/PVC film exhibited outstanding stability in harsh environments and can be easily regenerated by  $\text{NaBH}_4$  solution washing, which effectively prolongs its service life and reduces the operating cost. With the aid of a portable Raman spectrometer, on-site and *in situ* detection of multi-pesticide residues on apple surfaces has been achieved. Based on the unique properties, it is expected that the AuNPs/PVC film could bring the SERS technology closer to practical analysis, especially in the fields of food safety and environmental monitoring.

## Conflicts of interest

There are no conflicts of interest to declare.

## Acknowledgements

The authors acknowledge the financial support from the National Natural Science Foundation of China (Grant No. 21507124, 51578525 and 5153000136), and the Natural Science Foundation of Fujian Province (Grant No. 2015J05036).

## Notes and references

- 1 Y. Farina, M. P. Abdullah, N. Bibi and W. M. A. W. M. Khalik, *Food Chem.*, 2017, **224**, 55–61.
- 2 K. A. Lewis, J. Tzilivakis, D. J. Warner and A. Green, *Hum. Ecol. Risk Assess.*, 2016, **22**, 1050–1064.
- 3 X.-Y. Xu, B. Yan and X. Lian, *Nanoscale*, 2018, **10**, 13722–13729.
- 4 M. Govindasamy, U. Rajaji, S.-M. Chen, S. Kumaravel, T.-W. Chen, F. M. A. Al-Hemaid, M. A. Ali and M. S. Elshikh, *Anal. Chim. Acta*, 2018, **1030**, 52–60.
- 5 S. Pang, T. Yang and L. He, *TrAC, Trends Anal. Chem.*, 2016, **85**, 73–82.
- 6 R. A. Halvorson and P. J. Vikesland, *Environ. Sci. Technol.*, 2010, **44**, 7749–7755.
- 7 X. Liang, Y.-S. Wang, T.-T. You, X.-J. Zhang, N. Yang, G.-S. Wang and P.-G. Yin, *Nanoscale*, 2017, **9**, 8879–8888.
- 8 W. Zhao, S. Xiao, Y. Zhang, D. Pan, J. Wen, X. Qian, D. Wang, H. Cao, W. He, M. Quan and Z. Yang, *Nanoscale*, 2018, **10**, 14220–14229.
- 9 Y. C. Cao, R. Jin and C. A. Mirkin, *Science*, 2002, **297**, 1536–1540.
- 10 B. Liu, G. Han, Z. Zhang, R. Liu, C. Jiang, S. Wang and M.-Y. Han, *Anal. Chem.*, 2012, **84**, 255–261.
- 11 M. Mao, B. Zhou, X. Tang, C. Chen, M. Ge, P. Li, X. Huang, L. Yang and J. Liu, *Chem. – Eur. J.*, 2018, **24**, 4094–4102.
- 12 L. Polavarapu and L. M. Liz-Marzán, *Phys. Chem. Chem. Phys.*, 2013, **15**, 5288–5300.
- 13 A. Shiohara, J. Langer, L. Polavarapu and L. M. Liz-Marzán, *Nanoscale*, 2014, **6**, 9817–9823.
- 14 X. Lin, W.-L.-J. Hasi, S.-Q.-G.-W. Han, X.-T. Lou, D.-Y. Lin and Z.-W. Lu, *Phys. Chem. Chem. Phys.*, 2015, **17**, 31324–31331.
- 15 K. J. Si, P. Guo, Q. Shi and W. Cheng, *Anal. Chem.*, 2015, **87**, 5263–5269.
- 16 Z. Li, G. Meng, Q. Huang, X. Hu, X. He, H. Tang, Z. Wang and F. Li, *Small*, 2015, **11**, 5452–5459.
- 17 J. Chen, Y. Huang, P. Kannan, L. Zhang, Z. Lin, J. Zhang, T. Chen and L. Guo, *Anal. Chem.*, 2016, **88**, 2149–2155.
- 18 S. K. Bhunia, L. Zeiri, J. Manna, S. Nandi and R. Jelinek, *ACS Appl. Mater. Interfaces*, 2016, **8**, 25637–25643.
- 19 P. Wang, L. Wu, Z. Lu, Q. Li, W. Yin, F. Ding and H. Han, *Anal. Chem.*, 2017, **89**, 2424–2431.
- 20 H. Cui, S. Li, S. Deng, H. Chen and C. Wang, *ACS Sens.*, 2017, **2**, 386–393.
- 21 E. H. Koh, C. Mun, C. Kim, S.-G. Park, E. J. Choi, S. H. Kim, J. Dang, J. Choo, J.-W. Oh, D.-H. Kim and H. S. Jung, *ACS Appl. Mater. Interfaces*, 2018, **10**, 10388–10397.
- 22 G. Shi, M. Wang, Y. Zhu, Y. Wang and W. Ma, *Opt. Commun.*, 2018, **425**, 49–57.
- 23 L. B. Zhong, J. Yin, Y. M. Zheng, Q. Liu, X. X. Cheng and F. H. Luo, *Anal. Chem.*, 2014, **86**, 6262–6267.
- 24 F. Reincke, S. G. Hickey, W. K. Kegel and D. Vanmaekelbergh, *Angew. Chem., Int. Ed.*, 2004, **43**, 458–462.

- 25 Y. Wang, Y. Jin, X. Xiao, T. Zhang, H. Yang, Y. Zhao, J. Wang, K. Jiang, S. Fan and Q. Li, *Nanoscale*, 2018, **10**, 15195–15204.
- 26 B. Ren, G.-K. Liu, X.-B. Lian, Z.-L. Yang and Z.-Q. Tian, *Anal. Bioanal. Chem.*, 2007, **388**, 29–45.
- 27 L. Zhong, X. Zhou, S. Bao, Y. Shi, Y. Wang, S. Hong, Y. Huang, X. Wang, Z. Xie and Q. Zhang, *J. Mater. Chem.*, 2011, **21**, 14448–14455.
- 28 S. M. Ansar, F. S. Ameer, W. Hu, S. Zou, C. U. Pittman and D. Zhang, *Nano Lett.*, 2013, **13**, 1226–1229.